Growth and Field Emission Properties of ZnO Nanostructures Deposited by a Novel Pulsed Laser Ablation Source on Silicon Substrates

C. McLoughlin, P. Hough, J. Costello, E. McGlynn, J.P. Mosnier.

National Centre for Plasma Science and Technology (NCPST), School of Physical Sciences, Dublin City University, Glasnevin, Dublin 9, Ireland.

email: conor.mcloughlin2@mail.dcu.ie

Zinc oxide (ZnO) nanostructures were produced using a novel pulsed laser ablation apparatus comprising in-situ analysis of the plume by reflection time-of-flight mass spectrometry. Various morphologies of nano and microstructures were obtained for laser wavelengths of 1064 nm and 355 nm, and oxygen ambient pressures of 10^{-6} mbar and 10^{-2} mbar, respectively. None of the produced structures exhibited a particular type of self organisation whereas all of them showed low aspect ratios and good field emission properties. Optimum values of 5.2 $V\mu m^{-1}$ and 2060 were obtained for the turn-on field and Fowler-Nordheim enhancement factor, respectively, for deposited nano-tipped microstructures presenting a high coverage of the substrate. The experimental data showed that for a given laser wavelength, higher field enhancement factors were obtained for the samples grown at the lower pressure of 10^{-6} mbar. In these conditions, the deposited materials showed distinct nanostructuring and comparison with existing data showed the corresponding ablation plumes to contain $(ZnO)_n$ clusters, up to n=13. This work also shows that the electronic properties of the nanostructured ZnO produced in our conditions, as determined by the oxygen concentration during deposition, have an influence on the field emission properties in addition to the nanostructure morphology.

1. Introduction

There is currently an interest in the development of new field emission (FE) electron sources (cold cathodes) for use in future technologies such as miniature x-ray sources [1] or novel flat panel displays [2]. This has been driven by the relative failure of carbon nanotubes to reach the initially hoped for role as the ultimate cold cathode in spite of intensive research in the past decade [3,4].

Materials that readily form wire-like structures and have attractive electronic and material properties such as a low work function and high thermal stability are the obvious alternatives as they should form efficient and stable electron sources. One such material is the n-type semiconductor ZnO which has a direct wide band gap of 3.3 eV and is therefore a natural candidate for a surface with low electron affinity and work function, respectively. Furthermore, a substantial body of work has demonstrated in the past few years that ZnO is one of the most versatile materials for the fabrication of a plethora of nanostuctures, including nanorods and nanowires [5]. Thus, the FE properties of ZnO nanowires/nanopins were recognised some years ago [6] and continue to generate a considerable research effort e.g [7-9].

Recent works on the enhancement of field emission in nanostructured ZnO (nZnO) have also concentrated on the optimisation of its structural and electronic properties. Specific growth and fabrication methods have been developed by various authors to control and optimise the shape (sharp tip) and aspect ratio (height to width) of the nZnO emitters [10-12]. The optimisation of the electronic properties of field emitters by various surface treatments such as oxygen anneals, plasma treatments or ultra thin film deposition have also been investigated [13,14].

Pulsed laser deposition (PLD) has recently been recognised as a suitable technique for the production of FE device-quality ZnO nanowires/nanorods with the corresponding growth

mechanisms debated by the authors [15-17]. Here we have developed a novel laser ablation source in which the plume expands along a direction parallel to the substrate surface for deposition, thus allowing for simultaneous mass analysis with the help of an in-situ reflectron time-of-flight (ReTOF) mass spectrometer. We have studied the conditions in which optimised field emitters are produced and their possible relationship to both the processes of plume cluster formation and nZnO growth. We present the first results obtained with this new apparatus in the following sections of the paper.

2. Experimental details

Samples were grown using pulsed laser deposition, in a custom designed system schematically represented on figure 1. A Q-switched Nd:YAG laser was used either at the fundamental wavelength of 1064 nm or the wavelength of 355nm after frequency-tripling. The pulse width was about 6 ns for both wavelengths and the pulse repetition rate was 10 Hz. The fluence on target was kept fixed at ~7.7 J/cm^2 and obtained with a focal spot diameter of ~1mm at 45° incidence. The target was a 5N's purity ZnO ceramic disk, which was continuously rotated and translated during deposition so as to present a fresh surface for each laser shot. The depositions were carried out either in a high vacuum at a pressure of 10^{-6} mbar or in an oxygen ambient pressure of 10^{-2} mbar using a mass flow controller at a rate of 30 sccm. The depositions were performed at room temperature on phosphorus-doped n type Si (111) substrates placed parallel to the expansion of the plume, 5-7 cm away from the target (see figure 1). Substrates were degreased using an ultrasonic cleaning procedure prior to growth. 9,000 laser shots were used for each deposition.

The field emission properties of the deposited materials obtained from their I-V characteristics. The latter were measured in a vacuum chamber (base pressure 10^{-7} mbar) using an anode made of a flat polished aluminium plate mounted on a translation stage. The

assembly of the ZnO layer deposited on the conducting silicon substrate constituted the counter-electrode (cathode) and was positioned on a polytetrafluoroethylene (PTFE) block with an electrical feedthrough in its centre connected to the back of the substrate via conductive paste. A PTFE spacer of 100 μm thickness with a circular hole of diameter 2.5 mm in its centre was used to control the anode-cathode separation distance. The I-V characteristics were recorded using a computer controlled data acquisition system interfaced via GPIB to a SRS PS350 high voltage source (V) with a current feedback loop through a Keithley 6485 picoammeter (I).

The morphology of the grown materials were characterised by scanning electron microscopy (SEM).

3. Results and discussion

The samples morphologies are presented in Figure 2. The laser wavelength and growth pressures corresponding to samples of Fig. 2(a), (b), (c) and (d), hereafter referred to as samples (a), (b), (c) and (d), were 1064 nm at 10^{-2} mbar of oxygen , 1064 nm at 10^{-6} mbar, 355 nm at 10^{-2} mbar of oxygen and 355 nm at 10^{-6} mbar, respectively. All other experimental conditions were kept constant and described previously in section 2.

In the conditions of figure 2(a) long narrow microstructures are obtained, randomly distributed over the surface, with typical length of ~10 μm, no other structures are seen at greater magnifications. In Figure 2(b) both long (10-15 μm), narrow (0.2-0.5 μm) microstructures and nano-particles (150 nm) are observed. Both structures appear to be randomly distributed across the surface. The magnification in this case has been optimised to show more clearly the two types of structure. In the conditions of figure 2(c), one observes oblong nanostructures with average widths of 170 nm, average lengths of 350 nm while the average inter-structure spacing is typically 1 μm. Finally, in figure 2(d) we observe some self-organised growth of microstructures with dense packing on the surface and consistent heights and widths of ~1 μm and 0.5 μm, respectively.

The detailed in situ ReTOF plasma diagnostics of the ablation plumes corresponding to the growth conditions of samples (a)-(d) have been reported elsewhere [18] and the reader is referred to this reference for more detailed information about the corresponding mass spectra. We summarise here only the results relevant to the present study. For sample (a) no mass spectra for $(ZnO)_x$ clusters could be detected whereas the ablation plume of sample (b) showed mass spectra corresponding to Zn and ZnO with their dimers and cluster groups containing 6 zinc atoms and oxygen atoms varying between x = 6 to x = 9. The plume corresponding to sample (c) gave mass spectra showing the presence of Zn_x and $(ZnO)_x$ with

x = 1 and x = 2 only. Finally, mass spectra of the plume for deposition of sample (d) was rich in Zn_x and $(ZnO)_x$ clusters with x up to 13. Energy dispersive X-ray spectroscopy (EDX) was also performed on all samples and indicating the presence of Zn and O peaks for all the samples.

The I-V curves of samples (a)-(d) and their field emission properties obtained from Fowler-Nordheim (FN) plots are shown in figure 3(a) and 3(b), respectively. The turn-on field is determined by extrapolation of the I-V curve, as shown in figure 3(a). The turn on fields of samples (a), (b), (c) and (d) were ~ 11.8 $V\mu m^{-1}$, 7.5 $V\mu m^{-1}$, 6.0 $V\mu m^{-1}$ and 5.2 $V\mu m^{-1}$ respectively. Fitting the data using Fowler-Nordheim plots showed linear behaviour indicating the FN theory may be applied to obtain field enhancement factors. Field enhancement factors (β) for samples (a), (b), (c) and (d) were calculated using the slope of the linear graph as β = 1238, β = 1622, β = 1891 and β = 2060, respectively.

The above analysis shows that the most uniform nanostructure, that of sample (d), gives the most efficient turn on field with the highest field enhancement factor. This can be attributed in part to the favourable nanostructure morphology showing nanotips and also to the high surface coverage density of the sample. The FE properties of sample (c) can be explained by a downward trend from these favourable conditions due to a lower coverage density of oblong nanostructures yielding the second highest field enhancement factor of 1891 and lowest turn on field of 6.0 $V\mu m^{-1}$, respectively. Again this downward trend continues for sample (b) with a higher turn on field increasing to 7.5 $V\mu m^{-1}$ and a lower enhancement factor of 1622 compared to samples (c) and (d). This can be clearly related to the samples morphology comprised of particle-like nanostructures and long flat microstructures which both have low aspect ratios leading to a low enhancement factor. Finally, both the lowest enhancement factor and highest turn-on field values of 1238 and 11.8 $V\mu m^{-1}$ were observed

for sample (a) for which no nanostructured tips were present but only long microstructures lying flat on the surface.

We now relate these results to the plumes mass analyses summarised above. The ablation plumes corresponding to the deposition of samples (a) and (c) showed no cluster greater than the dimer of ZnO and a deficiency in nanostructured material on the substrate after deposition. On the other hand, the plume corresponding to the deposition of sample (b) contained $(ZnO)_x$ cluster groups with x up to 6, resulting in a mixture of long microstructures and an abundance of disordered particle-like nanomaterial. Similarly, the plume corresponding to the deposition of sample (d) showed a rich mass spectra of Zn_x and $(ZnO)_x$ with x up to 13 with a corresponding growth of a well-ordered nanostructured surface, clearly not present for the other depositions. From these observations, we conclude that there appears to exist a relationship between the presence of plume clusters and the formation of nanomaterial and thereby the FE properties of the nanomaterial. The plume containing the largest ZnO clusters lead to the formation of nanomaterial with the most favourable FE characteristics.

From Fig. 3, we also observe that the samples grown at 10^{-6} mbar have higher enhancement factors than the samples grown at 10^{-2} mbar in identical experimental conditions for a given laser wavelength. This can be explained in terms of the varying electronic properties of the deposits caused by the varying concentration of oxygen vacancies which is likely to result from the growth at different oxygen pressures. We note that in the case of ZnO nanorods Zhao et al. [13] have shown that the field emission properties are strongly influenced by the surface oxygen vacancy concentration. These effects can lead to the presence of surface states which can significantly affect the field emission properties via modification of the work function due to band bending effects [19,20]. However, in our experimental conditions where no oxygen anneals were applied, oxygen vacancies are likely to affect both the bulk and

surface electronic properties. A comparison of the values obtained here for the field enhancement factors and turn on fields with those of other works where the emphasis is on producing well-aligned, high-aspect ratio nanostructured ZnO [10-12], suggests that the field enhancement factor may be as much dependent on the ZnO material electronic properties as it is on the morphology.

4. Conclusions

ZnO nanostructures were produced via pulsed laser ablation by a novel apparatus comprising in-situ analysis of the plume by reflection time of flight mass spectrometry. Various morphologies of nano and microstructures were obtained as a function of the laser wavelength of 1064 nm or 355 nm and oxygen ambient pressures of 10^{-6} mbar or 10^{-2} mbar, respectively. All the grown structures produced no particular self organisation, with low aspect ratios. The I-V characteristics of all the samples were measured in vacuum and exhibited field emission behaviour compatible with the Fowler-Nordheim theory. The best values for the turn on field of $5.2 V\mu m^{-1}$ and enhancement factor β of 2060 were obtained for a pattern of nano-tipped microstructures deposited in the lower vacuum of 10^{-6} mbar using the 355 nm laser wavelength. A relationship was established between the presence of clusters in ablation plumes as obtained from ReTOF analyses and the deposition of nanostructured material. The plume of the sample exhibiting the best field emission properties was found to contain a range of $(ZnO)_x$ clusters with x up to 13. It was also observed that, for a given laser wavelength, the samples grown at 10^{-6} mbar have higher enhancement factors than the samples grown at 10^{-2} mbar which can be related to the concentration of oxygen vacancies in the material. Thus, the electronic properties of the nanostructured ZnO play as important a role as the structural properties in order to optimise the material field emission properties.

Acknowledgements

This work was sponsored by Science Foundation Ireland under grant number PHY041 and the HEA PRTLI IV programs of the 2nd National Development Program (NDP2).

References

[1] G.Z. Yue, Q. Qiu, Bo Gao, Y. Cheng, J. Zhnag, H. Shimoda, J.P. Lu and O. Zhou, Appl. Phys. Lett. 81 (2002) 355.

[2] J.D. Carey, Phil. Trans. R. Soc. Lond. A 361 (2003) 2891.

[3] S.R.P. Silva, J.D. Carey, X. Guo, W.M. Tsang, C.H.P. Poa, Thin Solid Films 482 (2005) 79.

[4] Jean-Marc Bonnard, Hannes Kind, Thomas Stöckli, Lars-Ola Nilsson, Solid State Electron. 45 (2001) 893.

[5] Zhong Lin Wang, J. Phys.: Condens. Matter 16 (2004) R829

[6] C.J. Lee, T.J. Lee, S.C. Lyu, Y. Zhang, H. RUh and H.J. Lee, Appl. Phys. Lett. 81 (2002) 3648

[7] R.T. Rajendra Kumar, E. Mc Glynn, C. Mc Loughlin, S. Chakrabarti, R.C. Smith, J.D. Carey, J.P. Mosnier and M.O. Henry, Nanotechnology 18 (2007) 215704.

[8] Jing Xiao, Yue Wu, Wei Zhang, Xin Nai, Ligang Yu, Shiqi Li and Gengmin Zhang, Appl. Surf. Sci. 254 (2008) 5426.

[9] Chi Li, Kai Hou, Wei Lei, Xiaobing Zhang, Baoping Wang and X.W. Sun, Appl. Phys. Lett. 91 (2007) 163502.

[10] D.F. Liu, Y.J. Xiang, X.C. Wu, Z.X. Zhang, L.F. Liu, L. Song X.W. Zhao, S.D. Luo, W.J. Ma, J. Shen, W.Y. Zhou, G. Wang, C.Y. Wang, S.S. Xie. Nano Lett. 6 (2006) 2375.

[11] Ning Zhang, Ke Yu, Yongsheng Zhang, Wei Bai, Ziqiang Zhu. Curr. Appl. Phys. 9 (2009) 34.

[12] Q. Ahsanulhaq, Jin-Hwan Kim and Yoon –Bong Hahn Nanotechnology 18 (2007) 485307

[13] Q. Zhao, X.Y. Xu, X.F. Song, X.Z. Zhang, D.P. Yu, C.P. Li, L. Guo.Appl. Phys. Lett. 88 (2006) 033102.

[14] L. Liao, J.C. Li, D.F. Wang, C liu, C.S. Liu, Q. Fu and L. X. Fan, Nanotechnology 16 (2005) 985.

[15] I. Ozerov, A.V. Bulgakov, D.K. Nelson, R. Castell, W. Marine, Appl. Surf. Sci. 247 (2005) 1.

[16] T. Okada, K. Kawashima, M. Ueda, Appl. Phys. A 81 (2005) 907;

[17] R. O'Haire, E. McGlynn, M.O. Henry, J.-P. Mosnier., Superlattice Microst. 42 (2007) 468

[18] Conor McLoughlin, Pádraig Hough, John Costello, Jean-Paul Mosnier, Applied Surface Science Particle diagnostics of a ZnO laser ablation plume for nanostructured material deposition, Appl. Surf. Sci. (2008), doi:10.1016/j.apsusc.2008.08.039.

[19] Z.W. Liu, C.K. Ong, T. Yu and Z.X. Shen, Appl. Phys. Lett. 88 (2006) 053110.

[20] Kungen Teii, Seiichiro Matsumoto, John Robertson. Appl. Phys. Lett. 92 (2008) 013115.

List of Figure Captions:

Figure 1: Schematic representation of the PLD system with in-situ ReTOF mass spectrometer.

Figure 2: SEM images of nanostructured thin films grown on Si (111) substrates with: (a) Laser operated at fundamental wavelength of 1064nm, a background pressure of 10^{-2}mbar, flow of O_2 at 30sccm and deposition time of 15 minutes, overhead image. (b) Laser operated at fundamental wavelength of 1064nm, a background pressure of 10^{-6}mbar and deposition time of 15 minutes, tilted image. (c) Laser wavelength 355nm, a background pressure of 10^{-2}mbar, flow of O_2 at 30sccm and a deposition time of 15 minutes, tilted image. (d) Laser wavelength 355nm, a background pressure of 10^{-6}mbar with 15 minutes deposition time, overhead image.

Figure 3: Field emission current as a function of applied field (a) and fits to Fowler-Nordheim equation (b) for all samples.

Figure 1

Click here to download high resolution image

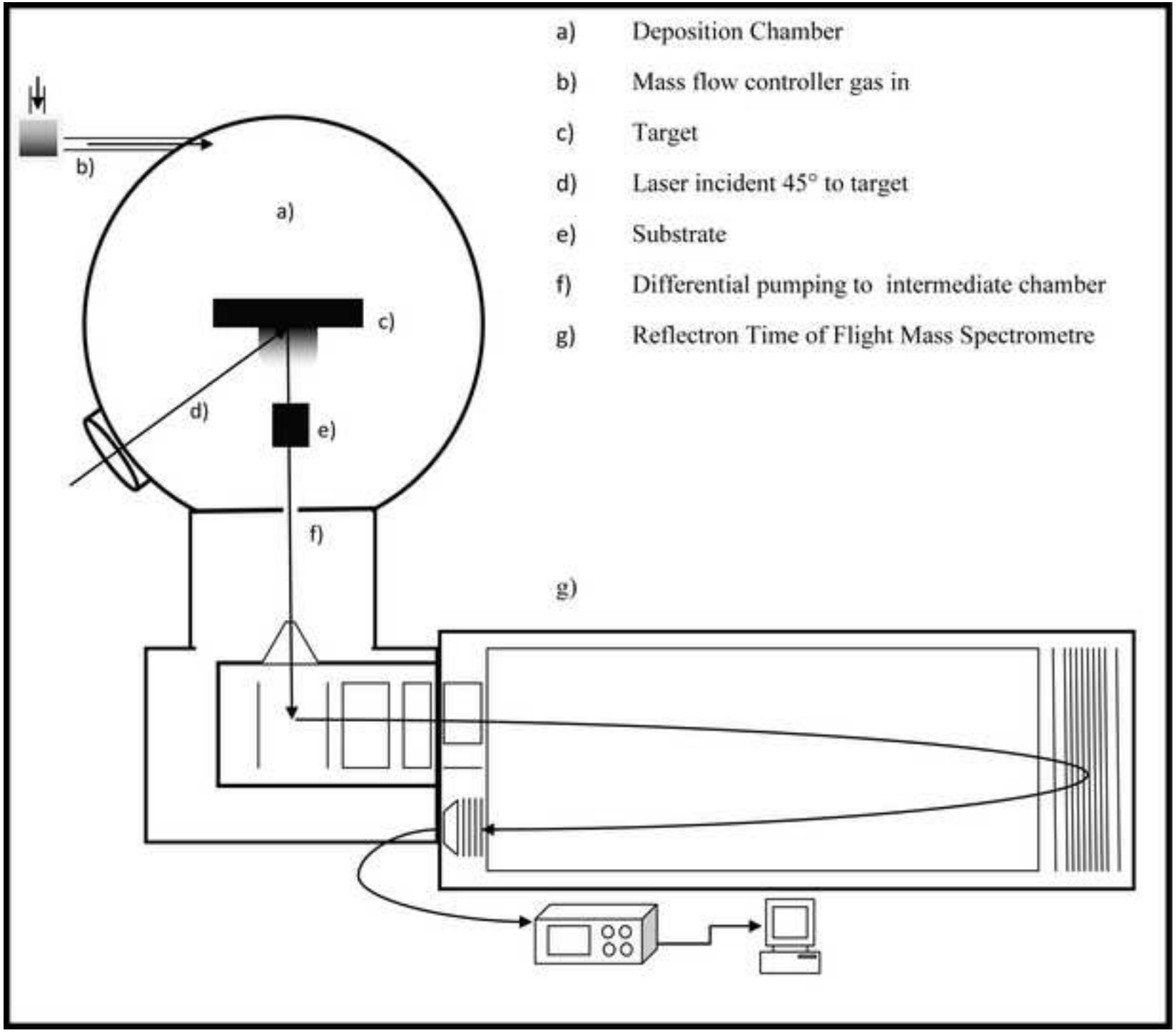

Figure 2

Click here to download high resolution image

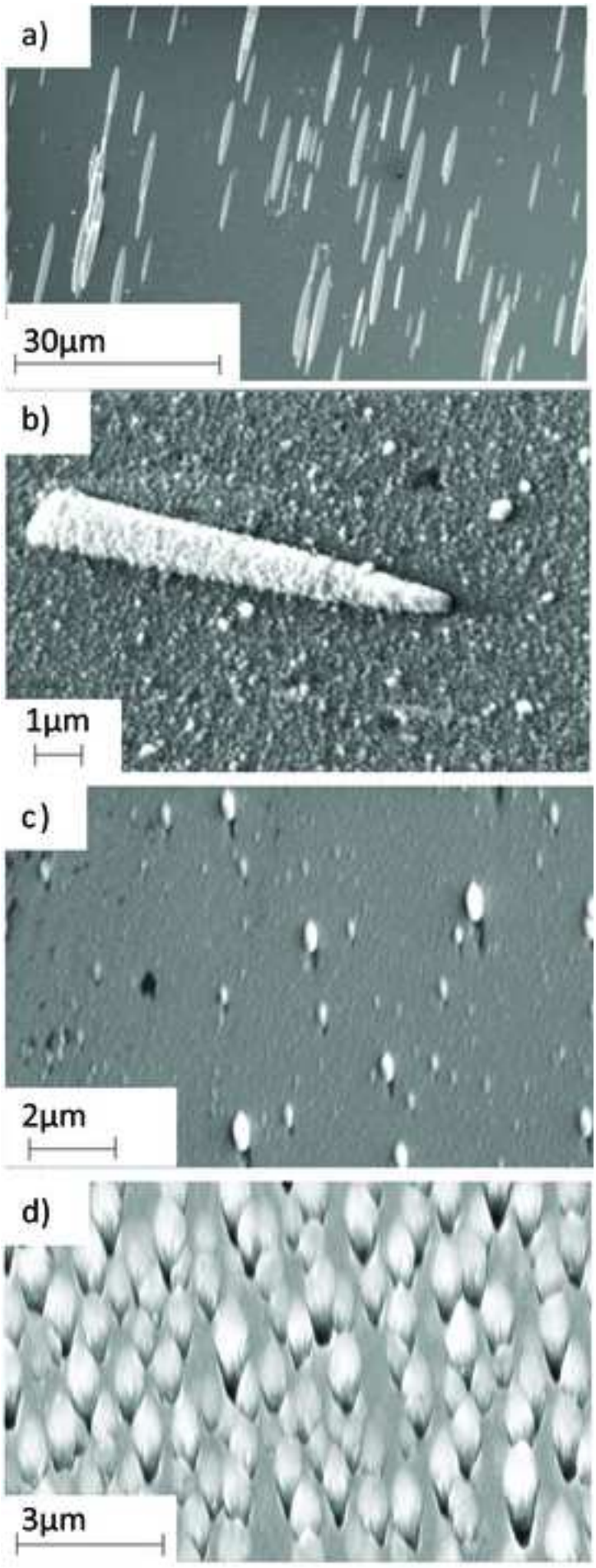

Figure 3

Click here to download high resolution image